Unpowered wireless transmission of ultrasound signals

2011 Smart Mater. Struct. 20 015017

(http://iopscience.iop.org/0964-1726/20/1/015017)

Smart Mater. Struct. **20** (2011) 015017 (7pp) doi:10.1088/0964-1726/20/1/015017

Unpowered wireless transmission of ultrasound signals

H Huang, D Paramo and S Deshmukh

Department of Mechanical and Aerospace Engineering, University of Texas at Arlington, 500 W. First Street, WH211, Arlington, TX 76019, USA

E-mail: huang@uta.edu

Received 23 September 2010, in final form 10 November 2010
Published 10 December 2010
Online at stacks.iop.org/SMS/20/015017

Abstract

This paper presents a wireless ultrasound sensing system that uses frequency conversion to convert the ultrasound signal to a microwave signal and transmit it directly without digitization. Constructed from a few passive microwave components, the sensor is able to sense, modulate, and transmit the full waveform of ultrasound signals wirelessly without requiring any local power source. The principle of operation of the unpowered wireless ultrasound sensor is described first, and this is followed by a detailed description of the implementation of the sensor and the sensor interrogation unit using commercially available antennas and microwave components. Validation of the sensing system using an ultrasound pitch–catch system and the power analysis model of the system are also presented.

(Some figures in this article are in colour only in the electronic version)

1. Introduction

Damage detection based on ultrasound is one of the most popular and well-researched non-destructive inspection schemes employed by many structural health monitoring (SHM) systems (Giurgiutiu 2008, Staszewski *et al* 2003). In general, there are two ways to implement an ultrasound SHM system, namely the pulse-echo method or the pitch–catch method. The pulse-echo method excites an ultrasound wave and senses its echoes using a single ultrasound transducer (Cincotti *et al* 1999). Defects are detected as additional echoes created due to the discontinuities in the ultrasound propagation medium. The pulse-echo systems are simple and inexpensive to implement because it only needs the access to one location on the structure. On the other hand, the interrogation distance of the pulse-echo method is relatively shorter since sensing the echo requires the round-trip travel of the ultrasonic wave. The pitch–catch method uses two ultrasound transducers; one for excitation and one for sensing. Detection of surface and near-surface cracks using the pitch–catch method, in which the amplitude and frequency of the ultrasonic waves are influenced by the existence of damage, has been extensively studied (Kessler *et al* 2002, Ip and Mai 2004, Toutanji 2000). For ultrasound detection, optical fiber-based (Culshaw *et al* 2008, Li *et al* 2009, Fomitchov *et al* 2000) and piezoelectric wafer sensors (Giurgiutiu 2008) are among the most preferred sensors. Majority of the optical fiber ultrasound sensors reported in the literature are based on one of the following interferometric techniques: Mach–Zehnder, Michelson, Fabry–Perot or Sagnac interferometers; although these optical fiber techniques possess higher flexibility, high strength and heat resistance, they are relatively expensive, complicated to implement on-site and highly susceptible to temperature fluctuations (Chen *et al* 2004). On the other hand, the applications of the piezoelectric wafer sensors are quickly being extended because of their compactness, light weight, low cost, and wide frequency range.

Recently, ultrasound tomography systems have been successfully developed for damage mapping in complex structures (Hay *et al* 2006, Rajgopalan *et al* 2006, Prasad *et al* 2004). Ultrasound tomography usually requires the implementation of a transducer array. One transducer is excited at one time while the rest of the transducers are used to acquire the ultrasound signals. By rotating the exciting transducer, a large set of ultrasound signals can be collected. An image reconstruction algorithm can then be applied to map out the sources that reflect/diffract ultrasound waves. Obviously, the resolution of the ultrasound tomography system depends on the number of transducers available. However, due to practical limitations, the number of such sensors that can be attached to a structure is limited (Prasad *et al* 2004). Alternatively, a method of mechanically scanning contact transducers over the entire surface was developed which utilizes fewer transducers (McKeon and Hinders 1999, Jansen *et al* 1990). Scanning tomography produced high spatial and image resolution, but the scanning hardware was too bulky and expensive. In addition, scanning with contact transducers is prone to errors from variations in coupling of the ultrasonic energy (Leonard *et al* 2002). To counter these coupling issues, air-coupled transducers that excite and receive guided waves at some lift-off from the test surface have been experimented (Popovics *et al* 2009, Wright *et al* 2005, Grandia and Fortunko 1995). However, the lift-off caused additional delays and attenuation, thus affecting the system performance. Ultrasound detection using an optical interferometer or a laser vibrometer is another non-contact ultrasound detection technique (Channels *et al* 2008, Murfin *et al* 2000, Huang *et al* 2008). Overall, non-contact ultrasound detection is very costly and less robust, making them more feasible for laboratory studies. Because of this reason, ultrasound SHM systems are still heavily relied on wired sensors. The weight penalty and maintenance concerns associated with wiring a large number of transducers have to be addressed for widespread field deployments of SHM systems.

Wireless sensors are attractive alternatives that can simplify the deployment of SHM systems and greatly reduce cable costs (Lynch and Loh 2006, Simonen *et al* 2004, Cho *et al* 2008). Furthermore, dense deployment of wireless sensors will increase the accuracy of the SHM techniques (Wu *et al* 2007, Caffrey *et al* 2004). The first wireless sensor for SHM was demonstrated by integrating wireless communications with accelerometers based on a low-power 8-bit Motorola 68HC11 microcontroller (Stracer and Kiremidjian 1998). However, the processing power of these sensors was not sufficient to execute sophisticated processing algorithms. To boost up the performance, a dual microcontroller core was designed where one microcontroller performs the data collection and the other performs sophisticated engineering analysis (Lynch 2002). The Berkley Mote Mica and Mica 2 are among the other popular platforms, however, the data sampling rate of these sensors is quite limited (Nitta *et al* 2005). Despite the tremendous efforts on wireless sensor research, very few are related to wireless ultrasound sensors (Grosse *et al* 2008, Liu and Yuan 2008, Zhao *et al* 2008). A major limitation of wireless ultrasound sensing technology is the fundamental incompatibilities between the high frequency of the ultrasound signals and the limit data throughput of existing wireless transponders. For example, transmitting the full waveform of a 1 MHz ultrasound signal sampled at 10 samples per cycle with a 16-bit resolution would require the wireless transponder to transmit at a rate of 160 Mega-bits s^{-1}. In contrast, the state-of-the-art wireless sensor based on the IEEE 802.11g protocol can only transmit a maximum data rate of 30 Mega-bits s^{-1} (Vassis *et al* 2005). This is about five times lower than the desired transmission rate. Due to this limitation, existing wireless ultrasound sensors have to resort to on-board data processing and only transmit the feature information. However, ultrasound signal processing usually requires large computation and thus consumes lots of power, which could drain out the battery quickly if the microprocessor ran continuously.

This paper presents a wireless ultrasound sensor that is fundamentally different from mainstream wireless sensors. Instead of having separate sensing, digitization, processing, and transmitting units, the present sensor uses frequency conversion to convert the ultrasound signal to a microwave signal and transmit it directly without digitization. More importantly, the frequency conversion and the transmission of the ultrasound-modulated signal can be achieved using a few passive microwave components. As a result, the sensor is able to sense, modulate, and transmit the full waveform of ultrasound signals wirelessly without requiring any local power source. The principle of operation of the sensor is explained first, followed by the discussions of the sensor design, sensor fabrication, and the derivation of the power-transmission model. Wireless transmission of the full waveform of ultrasound signals was demonstrated and characterized using an ultrasound pitch–catch system. The power-transmission model of the wireless ultrasound sensing system was experimentally validated.

2. Principle of operation

The wireless ultrasound sensing system is based on the principle of frequency conversion using a frequency mixer. A frequency mixer is a nonlinear microwave device that converts a high frequency, i.e. the RF frequency, to a low intermediate frequency, i.e. the IF frequency, and vice versa. A frequency mixer has three ports, the local oscillator (LO) port, the RF port, and the IF port. For the up-conversion operation, the input signals are the LO signal and the IF signal. The frequency of the output signal, i.e. the RF signal, is related to the frequencies of the LO and the IF signals as

$$f_{\mathrm{RF}} = f_{\mathrm{LO}} \pm f_{\mathrm{IF}}. \tag{1}$$

For the down-conversion operation, the frequency mixer takes the RF signal and the LO signal as the inputs and produces an IF signal with a frequency of

$$f_{\mathrm{IF}} = f_{\mathrm{RF}} \pm f_{\mathrm{LO}}. \tag{2}$$

Because ultrasound waves in general have frequencies of a few tens of kilohertz to a few megahertz, direct wireless transmission of the ultrasound signals would require an antenna so big that makes it impractical to be implemented at the sensor level. In this application, we use a passive frequency mixer to up-convert the ultrasound signal to the microwave frequency so that it can be transmitted wirelessly using a compact antenna. Once the wireless signal is received, the ultrasound signal can be down-converted back to its original frequency.

An illustration of the wireless ultrasound sensing system is shown in figure 1. It consists of two major subsystems; the wireless sensor node and the sensor interrogation unit (SIU) located at a distance away from the sensor. The sensor node consists of four components, namely two antennas (sensor Rx and Tx), a frequency mixer, and a piezo wafer sensor. The antennas and the frequency mixer form a wireless transponder that up-converts the ultrasound signal to a microwave signal and transmits the ultrasound-modulated microwave signal wirelessly. The piezo wafer sensor converts the mechanical

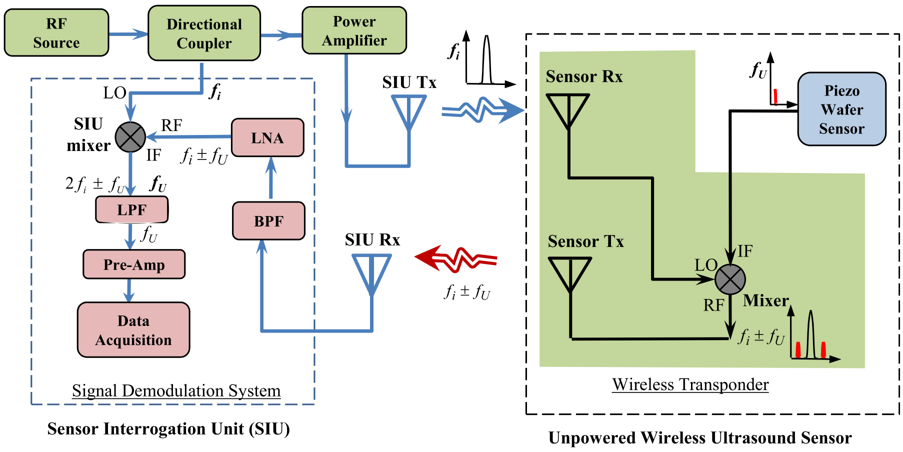

Figure 1. Unpowered wireless ultrasound sensor and associated sensor interrogation unit.

ultrasound motion to an electrical signal f_U. To up-convert the ultrasound signal to the microwave frequency, an interrogation microwave signal f_i, i.e. the LO signal, is received by the sensor Rx antenna. Mixing the ultrasound signal and the LO signal using the frequency mixer produces an ultrasound-modulated microwave signal $f_i \pm f_U$. This modulated signal, encoded with the ultrasound information, is transmitted using the sensor Tx antenna. Since all components at the sensor level are passive, i.e. they do not need a local power supply, unpowered wireless transmission of the ultrasound signal is thus achieved. The SIU broadcasts the microwave interrogation signal f_i to the sensor node and demodulates the received signal $f_i \pm f_U$ to recover the ultrasound signal f_U. It consists of two antennas (SIU Rx and Tx), a signal generator, and a signal demodulation system. The microwave signal generated by the signal generator is split into two signals using a directional coupler. One part of the signal serves as the LO signal for the down-converting mixer. The other part of the signal, serving as the interrogation signal f_i, is amplified by a power amplifier, broadcasted through the SIU Tx antenna, and received by the sensor Rx antenna. The ultrasound-modulated signal $f_i \pm f_U$ is received by the SIU Rx antenna and passed on to the signal demodulation system to recover the ultrasound signal. The signal demodulation system first filters the received signal using a bandpass filter (BPF), amplifies the received modulated signal using a low-noise amplifier (LNA), and down-converts it using the frequency mixer. Since the LO signal has the same frequency as the interrogation signal, the IF port of the down-converting mixer produces a signal with frequency components at f_U and $2f_i \pm f_U$. Filtering this IF signal using a low pass filter (LPF) recovers the ultrasound signal f_U. After filtering, the ultrasound signal can be amplified again and acquired using a conventional wired data acquisition system.

3. Design and fabrication of the wireless transponder

The wireless transponder at the sensor node was constructed by soldering two 0 dBi chip antennas (Antenna Factor ANT-2.4-Chp-x, 6.6 mm long, 2.3 mm wide, and 1mm thick) and a frequency mixer (Minicircuits, ZX05-73L-S+) on a printed circuit board (Roger 4350B, 0.5 mm thick, and 50 mm × 25 mm). The layout of the transponder board, designed using an Electromagnetic Simulation Tool, Sonnet Pro, is shown in figure 2(a). The two chip antennas were designed to have a 90° polarization differences to reduce the cross-talk between these two antennas. The board material is a laminate with a dielectric substrate sandwiched between two thin copper coatings (12.7 μm thick). One side of the copper coating was milled using a CNC machine to produce the copper traces, which serve as the microstrip transmission lines that electrically connect the two chip antennas and the mixer. The width of the copper trace was calculated from its characteristic impedance z_0, the dielectric constant of the substrate material ε, the height of the substrate h, and the copper thickness t as

$$w = \frac{7.4625\,h}{\mathrm{e}^{(Z_0\sqrt{0.475\varepsilon+0.67}/60)}} - 1.25t. \qquad (3)$$

For a substrate thickness of 483 μm, a copper thickness of 12.7 μm, a dielectric constant of 3.66, and a characteristic impedance of 50 Ω, the trace width is calculated to be 1 mm. The traces are chamfered at an angle of 45°, at all perpendicular turns, to maintain a characteristic impedance of 50 ohms throughout the length. For shielding purpose, the copper coating besides the copper traces are connected to the copper coating on the back side of the substrate, i.e. the ground plane, by drilling a few holes on the laminate and filling the holes with solder (see figure 2(b)). The distance between the microstrip traces and the ground plane is not very crucial. A rule of thumb is to keep this distance approximately equal to (or greater than) the trace width. A larger gap will reduce the shielding efficiency. According to the antenna manufacturer's instructions, the area underneath the chip antennas should be free of any components, traces or planes. Therefore, the copper coatings on both sides of the laminate that are underneath the chip antenna were etched off. After the board was machined, the chip antennas and the frequency mixer were soldered on the microstrip traces.

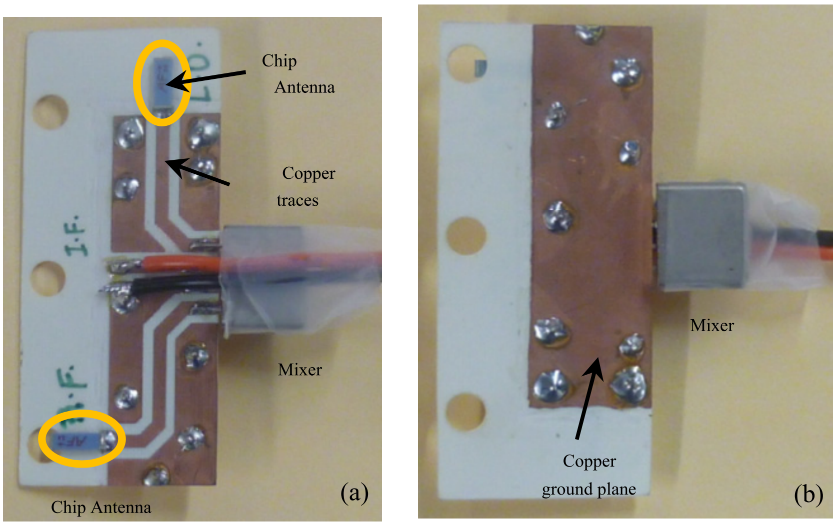

Figure 2. Wireless transponder; (a) front view with chip antennas and mixer mounted on the traces; (b) back view showing the ground plane.

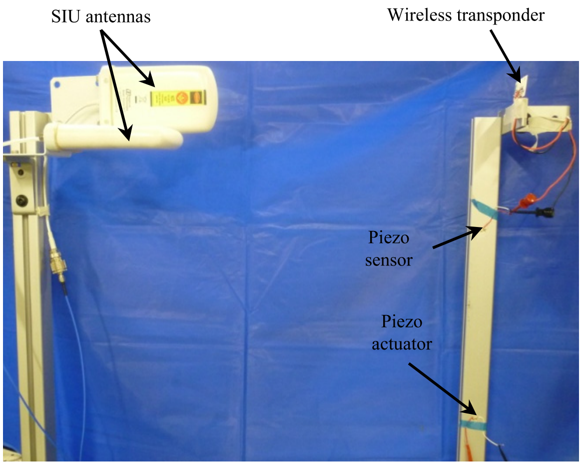

Figure 3. Wireless ultrasound sensing system.

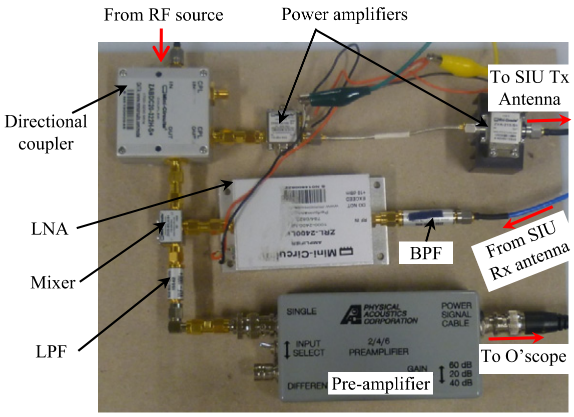

Figure 4. Signal demodulation system.

4. Hardware implementation and experiment setup

The implementation of the passive wireless ultrasound sensing system is shown in figure 3. An ultrasound pitch–catch system was implemented on an aluminum channel by installing two piezo wafer sensors; one for actuation and the other for sensing. The wall thickness of the aluminum channel is 2 mm. The two piezo wafer sensors (APC 850, 7 mm in length and width, 250 μm in thickness) were placed at a distance of 279 mm apart. A 5.5 cycle tone-burst signal with peak-to-peak amplitude of 10 V was generated by a signal generator (Agilent 33250A) and supplied directly to the piezo wafer actuator to excite Lamb waves. Two wideband 8 dBi log periodic antennas (Hyperlink Technologies, HG2458-08LP) were aligned to have the same polarization as their counterpart antennas at the sensor node. The distance between the SIU and the sensor was 0.6 m.

The SIU signal demodulation system was assembled using commercially available components shown in figure 4. A directional coupler (Minicircuits, ZABDC20-322H-S+) separates the microwave signal supplied by a signal generator (Agilent, E4421B) into two signals. The large signal from the 'output' port was connected to the LO port of the down-converting mixer (Minicircuits, ZX05-73L-S+). The small signal output from the 'CPL out' port was amplified using two power amplifiers (Minicircuits, ZX60-6013E-S+ and ZVA-213-S+) to reach a power level of around 24 dBm. This amplified microwave signal, serving as the interrogation signal f_i, was supplied to the SIU Tx antenna and broadcasted to the wireless sensor node. The ultrasound-modulated microwave signal, received by the SIU Rx antenna, was first bandpass-filtered (Minicircuits, VBFZ-2575-S+), amplified using a LNA (Minicircuits, ZRL-2400LN+), and finally supplied to the RF port of the down-converting mixer. The demodulated ultrasound signal, i.e. the IF output of the mixer, was filtered using a low pass filter (Minicircuits, VLF-1000+) and amplified using a pre-amplifier (Physics Acoustics Corporation 2/4/6 preamplifier). Finally, the output of the pre-amplifier was acquired using a high speed oscilloscope (LeCory SDA 760Zi).

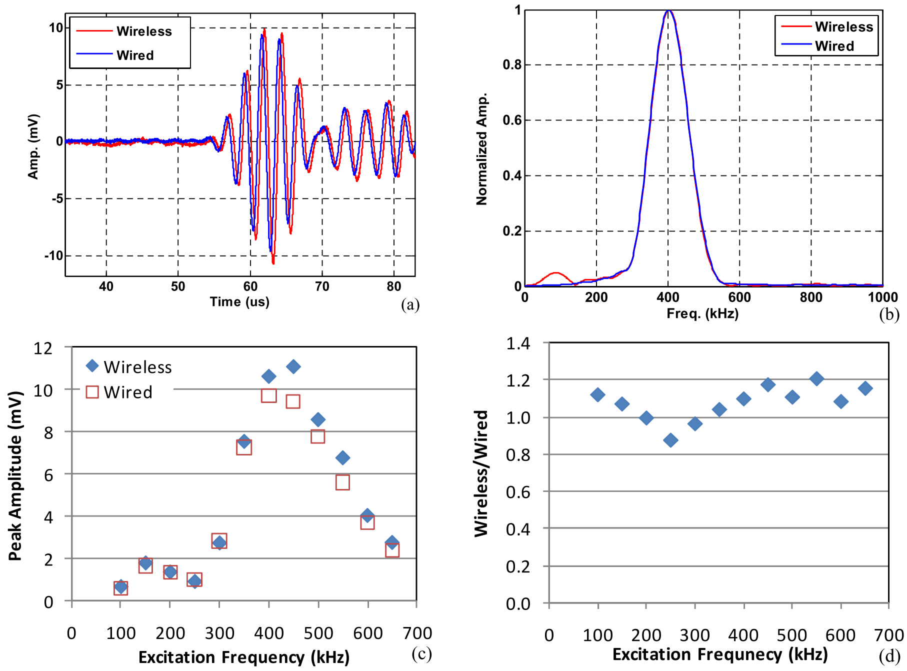

Figure 5. Comparison of wired and wirelessly acquired ultrasound signals at 400 kHz excitation frequency; (a) acquired signals; (b) normalized frequency spectra of the first arriving wavepackets; (c) wireless versus wired signal at different excitation frequencies; (d) ratio between peak values of wired and wirelessly acquired signals at different excitation frequencies.

5. Power-transmission model

Assuming the sensor Rx antenna is placed at a distance d from the SIU Tx antenna, the power of the signal received by the sensor Rx antenna can be calculated from the Friis transmission equation (Balanis 2005) as

$$P_s = \frac{P_i G_h G_s \lambda^2}{(4\pi d)^2}, \qquad (4)$$

where P_i is the interrogation power, G_h and G_s are the gains of the SIU Tx and sensor Rx antennas, and λ is the microwave wavelength. Denoting the root-mean-square (RMS) amplitude of the output of the piezo wafer sensor as V_U, the RMS amplitude of the ultrasound-modulated signal is

$$V_m = V_s V_U = \sqrt{P_s R} V_U = \sqrt{P_i G_h G_s R} \frac{\lambda}{4\pi d} V_U \qquad (5)$$

where R is the impedance of the frequency mixer and V_s is the RMS amplitude of the microwave signal received by the sensor node. The power of the ultrasound-modulated signal, taking the insertion loss of the mixer A_{mixer1} into consideration, is

$$P_m = A_{mixer1}\left(\frac{V_m^2}{R}\right) = \frac{A_{mixer1} P_i G_h G_s \lambda^2}{(4\pi d)^2} V_U^2. \qquad (6)$$

The power of the modulated signal P_r, received by the SIU Rx antenna, is again calculated from the Friis transmission equation as

$$P_r = \frac{P_m G_h G_s \lambda^2}{(4\pi d)^2} = \frac{A_{mixer1} P_i (G_h G_s)^2 \lambda^4}{(4\pi d)^4} V_U^2. \qquad (7)$$

Denoting the gain of the LNA as A_{LNA} and the gain of the pre-amplifier as A_{amp}, the RMS amplitude of the recovered ultrasound signal is

$$V_r = \sqrt{A_{amp} P_{IF} R} = \sqrt{A_{amp} A_{LNA} A_{mixer1} A_{mixer2} P_i P_{LO}} \times \frac{G_h G_s \lambda^2}{(4\pi d)^2} R V_U, \qquad (8)$$

where A_{mixer2} is the insertion loss of the down-converting mixer and P_{LO} is the power of the LO signal.

6. Experimental results and analysis

Wireless transmission of the full waveform of ultrasound signals was demonstrated and characterized using the ultrasound pitch–catch system shown in figure 3. The interrogation signal had a frequency of 2.4 GHz and the power output of the signal generator was 5 dBm. The ultrasound excitation signal was a 5.5 cycle Hanning windowed tone-burst signal with a peak-to-peak amplitude of 10 V and a repetition period of 10 ms. The ultrasound signals acquired by the oscilloscope was averaged over 100 sweeps. For an excitation burst frequency of 400 kHz, the comparison between the signals collected through the wireless channel and the wired piezo sensor wafer are shown in figure 5. With a pre-amplifier gain of 40 dB, the signal collected using the wireless means has a similar amplitude as that of the ultrasound signal directly acquired from the piezo wafer sensor. The wired signal shown in figure 5(a) has a 180° phase difference from the as-acquired wired signal. This phase difference and the slight time delay between the wired and wireless signals are due to the pre-amplifier. The first arriving wavepackets were extracted from the signals using a rectangular window between

Table 1. Comparison of calculated and measured signal power at different stages. (Note: measurement data compensated for cable/connector loss.)

Measurands	Supplied (dBm)	Calculated (dBm)	Measured (dBm)
Interrogation signal (P_i)	24.43		
Sensor received signal (P_s)		−3.32	−4.5
Ultrasound signal (P_U)	−20		
Ultrasound-modulated signal (P_m)		−37.5	−36.5
SIU received modulated signal (P_r)		−64.4	−62.9
Signal amplified by LNA		−37.9	−37.9
Down-converting LO signal (P_{LO})	3.45		
Recovered ultrasound signal (P_{ru})		−47.5	−50

50 and 70 μs. By performing fast Fourier transformation (FFT) on the first arriving wavepackets, we can compare the signal-to-noise ratio (SNR) of these two sets of data. As shown in figure 5(b), the two signals have almost identical frequency spectra except the wireless signal has a small bulge around 100 kHz. We have also compared the peak value of the 1st arriving wavepacket at different excitation frequencies. The wireless signal matched relatively well with the wired signal, as shown in figure 5(c). Between 200 and 300 kHz, the ultrasound waveform was not very well defined and the amplitude was very low. These may be the reason that the ratio between the peak amplitude of the wireless and wired signal is slightly lower at these frequencies than those at other frequencies. Overall, the wireless ultrasound sensing system has a relatively flat bandwidth (see figure 5(d)).

In order to validate the power-transmission model, the wireless transponder was assembled using discrete components, i.e. two prototype chip antennas and a packaged frequency mixer (see figure 6). These components were connected through SMA connectors so that step-to-step power measurements can be carried out. A 500 kHz continuous sinusoidal signal with a power of −20 dBm, equivalent to a 20 mV RMS amplitude for a 50 Ω impedance, was generated by a signal generator and supplied to the IF port of the sensor mixer to imitate the ultrasound signal. Again the signal generator was set at a frequency of 2.4 GHz and a power level of 5 dBm, which resulted in an interrogation signal of 24.43 dBm and an LO signal of 3.45 dBm for the SIU mixer. The signal power was measured from the spectra of the signals acquired by the high speed oscilloscope sampled at 20 Giga samples per second. The power measurements have an uncertainty of 2.7 dB for the microwave signals and 0.6 dB for the ultrasound signal, due to the cable and connector loss. The measurement data were therefore increased by the corresponding amount to compensate for these losses. The measured and calculated signal powers at different stages differed by a few decibels, which is likely contributed by the uncertainties of the cable/connector losses (see table 1). The main loss is contributed by the wireless transmission of the interrogation signal and the ultrasound-modulated signal. Each path contributed about −28 dB of loss at a distance of 0.6 m between the two antennas. To reduce these losses, high gain antennas, such as patch antennas for the sensor node and a dual-polarized horn antenna for the SIU, can be used. Increasing the gains of the antennas and the interrogation power will enable wireless interrogation of the ultrasound sensor at a larger distance. The insertion losses of the mixers appear to be insignificant, even though the sensor mixer was operating at a LO signal that was way below the specified level. Compared with the wireless transponder with discrete components, the wireless transponder constructed on the PCB has an additional 10 dB loss. Better design and fabrication of the board can reduce this loss.

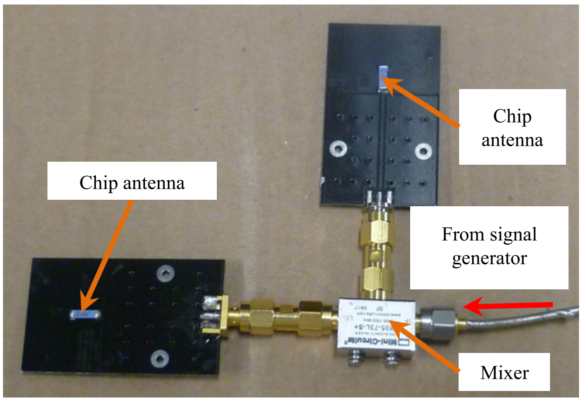

Figure 6. Wireless transponder with discrete components.

7. Conclusions

We have demonstrated an unpowered wireless ultrasound sensor based on the principle of frequency conversion. The design and implementation of the wireless ultrasound sensor are presented and the performance of the wireless ultrasound sensing system was characterized. A power-transmission model for this system was established and validated.

Acknowledgments

The authors gratefully acknowledge the support of this project by the National Science Foundation CAREER award (CMMI-0846074, Program Manager Shih-chi Liu) and the Texas Ignition fund.

References

Balanis C A 2005 *Antenna Theory: Analysis and Design* 3rd edn (New York: Wiley–Interscience)

Caffrey J *et al* 2004 Networked sensing for structural health monitoring *4th Int. Workshop on Structural Control (Columbia University)*

Channels L, Chakraborty D, Simon D, Kovvali N, Spicer J, Papandreou-Suppappola A, Cochran D, Peralta P and Chattopadhyay A 2008 Ultrasonic sensing and time frequency analysis for detecting plastic deformation in an aluminium plate *Proc. SPIE* **6296** 62960P-1

Chen R, Fernando G F, Butler T and Badcock R A 2004 A novel ultrasound fiber optic sensor based on a fused-tapered optical fiber coupler *Meas. Sci. Technol.* **15** 1490–5

Cho S, Yun C B, Lynch J P, Zimmerman A T, Spencer B F and Nagayama T 2008 Smart wireless sensor technology for structural health monitoring of civil structures *Steel Struct.* **8** 267–75

Cincotti G, Cardone G, Gori P and Pappalardo M 1999 Efficient transmit beamforming in pulse-echo ultrasonic imaging *IEEE Trans. Ultrason. Ferroelectr. Freq. Control* **46** 1450–8

Culshaw B, Thursby G, Betz D and Sorazu B 2008 The detection of ultrasound using fiber-optic sensors *IEEE Sensors* **8** 1360–7

Fomitchov P A, Krishnaswamy S and Achenbach J D 2000 Extrinsic and intrinsic fiber optic Sagnac ultrasound sensors *Optic Eng.* **39** 1972–84

Giurgiutiu V 2008 *Structural Health Monitoring with Piezoelectric Wafer Active Sensors* (Burlington, MA: Academic)

Grandia W A and Fortunko C M 1995 NDE applications of air-coupled ultrasonic transducers *Proc. IEEE Ultras. Symp.* vol 1 pp 697–709

Grosse C, McLaskey G, Bachmaier S, Glacer D S and Kruger M 2008 A hybrid wireless sensor network for acoustic emission testing in SHM *Proc. SPIE* **6932** 693238

Hay T R, Royer R L, Gao H, Zhao X and Rose J L 2006 A comparison of embedded sensor Lamb wave ultrasonic tomography approaches for material loss detection *Smart Mater. Struct.* **15** 946–51

Huang H, Pamphile T and Derriso M 2008 The effect of actuator bending on Lamb wave displacement fields generated by a piezoelectric patch *Smart Mater. Struct.* **17** 055012

Ip K and Mai Y 2004 Delamination detection in smart composite beams using Lamb waves *Smart Mater. Struct.* **13** 544–51

Jansen D P, Hutchins D A and Young R P 1990 Ultrasonic tomography using scanned contact transducers *J. Acoust. Soc. Am.* **93** 3242–9

Kessler S, Spearing S M and Soutis C 2002 Damage detection in composite materials using lamb wave method *Smart Mater. Struct.* **11** 269–78

Leonard K R, Malyarenko E and Hinders M 2002 Ultrasonic Lamb wave tomography *Inverse Problems* **18** 1795–808

Li F, Murayama H, Kageyama K and Shirai T 2009 Doppler effect-based fiber-optic sensor and its application in ultrasonic detection *Opt. Fiber Technol.* **15** 296–303

Liu L and Yuan F G 2008 Wireless sensors with dual-controller architecture for active diagnosis in structural health monitoring *Smart Mater. Struct.* **17** 025016

Lynch J P 2002 Decentralization of wireless monitoring and control technologies for smart civil structures *PhD Dissertation* Stanford University

Lynch J P and Loh K 2006 A summary review of wireless sensors and sensor networks for structural health monitoring *Shock Vib. Dig.* **38** 91–128

McKeon J C P and Hinders M K 1999 Parallel projection and crosshole Lamb wave contact scanning tomography *J. Acoust. Soc. Am.* **106** 2568–77

Murfin A S, Soden R A J, Hatrick D and Dewhurst R J 2000 Laser-ultrasound detection systems: a comparative study with Rayleigh waves *Meas. Sci. Technol.* **11** 1208–19

Nitta Y, Nagayam T, Spencer J and Nishitani A 2005 Rapid damage assessment for the structures utilizing smart sensor MICA2 MOTE *Structural Health Monitoring Proc. 5th IWSHM* pp 283–90

Popovics J, Gibson A, Hall K and Shin S W 2009 Developments in air-coupled contactless sensing for concrete *Non-Destructive Testing in Civil Engineering (Nantes, France)*

Prasad S M, Balasubramaniam K and Krisnamurthy C V 2004 Structural health monitoring of composite structure using Lamb wave tomography *Smart Mater. Struct.* **13** N73–9

Rajgopalan J, Balasubramaniam K and Krisnamurthy C V 2006 A phase reconstruction algorithm for Lamb wave based structural health monitoring of anisotropic multilayered composite plates *J. Acoust. Soc. Am.* **119** 872–8

Simonen J T, Andringa M, Grizzle K, Wood S and Neikirk D 2004 Wireless sensors for monitoring corrosion in reinforced concrete members *Proc. SPIE* **5391** 587–96

Staszewski W, Boller C and Tomlinson G 2003 *Health Monitoring of Aerospace Structures* (Chichester: Wiley)

Stracer E G and Kiremidjian A S 1998 A modular, wireless damage monitoring system for structures *Phd Thesis* Stanford Univeristy

Toutanji H 2000 Ultrasonic wave velocity signal interpretation of simulated concrete bridge decks *Mater. Struct.* **33** 207–15

Vassis D, Kormentzas G, Rouskas A and Maglogiannis I 2005 The IEEE 802.11g standard for high data rate WLANs *IEEE Network* **19** 21–6

Wright W, Ingleby P and O'Sullivan I 2005 Air-coupled through-transmission fan-beam tomography using divergent capacitive ultrasonic transducers *IEEE Trans. Ultrason. Ferroelectr. Freq. Control* **52** 2384–94

Wu J, Yuan S, Zhao X, Yin Y and Ye W 2007 A wireless sensor network node designed for exploring a structural health monitoring application *Smart Mater. Struct.* **16** 1898–906

Zhao X, Qian T, Popovic Z, Zane R and Mei G 2008 Wireless ultrasonic transducer network for structural health monitoring of an aircraft wing *17th World Conf. on Nondestructive Testing (Shanghai)*